Atmospheric Research 246 (2020) 105112

Contents lists available at ScienceDirect

Atmospheric Research

journal homepage: www.elsevier.com/locate/atmosres

Projections of future meteorological drought events under representative concentration pathways (RCPs) of CMIP5 over Kenya, East Africa

Guirong Tan[a,*], Brian Ayugi[a,*], Hamida Ngoma[a], Victor Ongoma[a,b]

[a] Key Laboratory of Meteorological Disaster, Ministry of Education (KLME)/Joint International Research Laboratory of Climate and Environment Change (ILCEC)/ Collaborative Innovation Center on Forecast and Evaluation of Meteorological Disasters (CIC-FEMD), Nanjing, University of Information Science and Technology, Nanjing 210044, China

[b] School of Geography, Earth Science and Environment, University of the South Pacific, Laucala Campus Private Bag, Suva, Fiji

ARTICLE INFO

Keywords:
Drought
Standardized precipitation index (SPI)
Rossby centre atmospheric regional climate model (RCA4)
Future projections
Kenya

ABSTRACT

Understanding future evolution of drought scenario across localized domains remains an imperative process in bid to adapt tailor suit innovative solutions to drought risks and their impacts. The present study examines drought events by characterizing the trend, intensity, severity and frequency based on Standardized Precipitation Index (SPI), over Kenya, East Africa for near future (2010–2039), mid-century (2040–2069), and late century (2070–2100). The study utilizes Multi-model mean ensemble (MME) of five selected regional climate models (RCMs). Further, the models are bias corrected based on a quantile mapping bias corrected algorithm in order to minimize possible bias for accurate projections. The changes in annual and seasonal precipitation over Kenya is examined in order to associate with changes in drought occurrence. Results demonstrate positive shift, indicating an increase in projected rainfall change during all the three timescales. Projections of possible future meteorological drought events under RCPs scenario over study locale was conducted using SPI. The results demonstrate relatively better performance of biased corrected MME derived from Rossby Centre regional climate model (RCA4) in simulating drought indices over the Kenya. The MME projections for drought duration show an increase in moderate drought incidences with fewer incidences of extreme events across the RCP4.5 and 8.5 scenarios respectively. However, the duration of occurrences varies from one region to another with most hotspots located around northeastern sides of the country. Examination of projected changes in drought frequency and severity depict an occurrence of severe to extreme drought incidences that are expected to intensify during the near future time slice while overall projections show that more wet scenarios is depicted, with fewer cases of drought expected to occur during mid and towards end of the century of projection period. The study calls for enactment of appropriate mitigation measures to cope with possible scenarios of drought risks over Kenya in the future.

1. Introduction

The steady increase in the emission of greenhouse gases (GHGs) across the globe will continue to exacerbate the observed global warming. This influences the occurrence of extreme events that have adverse impacts on global economy, human health, infrastructure and ecosystems. Most noticeable climate extremes over the last few years such as; 2018 German heatwaves, 2018 heavy torrents in Japan, 2018 Typhoon Mangkhut in Philippines, and 2019/2020 Australian wild fires among others will continue to reoccur if global community maintain "business as-usual" emission scenario of the GHGs. Moreover, devastating events such as drought and pluvial scenarios are likely to increase in frequency and severity in most regions as projected in the recent studies (Sheffield and Wood, 2007, Sheffield and Eric, 2008; Dai, 2013; Huang et al., 2016; Spinoni et al., 2020).

For instance, Duffy et al. (2015) projects an increase in drought events over eastern Amazon ecosystems which is described as the "lungs of the earth". This poses threat to the survival of humanity and the larger ecosystem since the droughts over this region may intensify fire occurrences, tree mortality, and emissions of carbon to the atmosphere across large domains of Amazonia. Similar projections are noted over North America region (Wehner et al., 2011; Jung and Chang, 2012; Ahmadalipour et al., 2017a); Sub-Saharan Africa (Gidey et al., 2018; Nguvava et al., 2019; Naik and Abiodun, 2020); larger basins in China and Asian domains (Prudhomme et al., 2014; Wang et al., 2018; Huang et al., 2018); and snowpack regions (Mote et al., 2018; Huning

* Corresponding authors.
E-mail addresses: tanguirong@nuist.edu.cn (G. Tan), ayugi.o@gmail.com (B. Ayugi).

https://doi.org/10.1016/j.atmosres.2020.105112
Received 4 April 2020; Received in revised form 10 June 2020; Accepted 18 June 2020
Available online 20 June 2020
0169-8095/

and AghaKouchak, 2018). The projected drought scenarios will lead to the expansion of global dryland with some studies recording an increase of drylands from current 10–23% of a total land surface to approximately, 50–56% over the global biospherics component. (Huang et al., 2016). The resultant impact of the projected drought and aridity index over already fragile ecosystems will likely trigger some localized feedbacks such as increased occurrence of dust events or alteration of surface water table (Skiles et al., 2018).

Despite the projected intensification of drought occurrence across various regions globally, there are still large uncertainties regarding observed global scale trends in droughts (Burke and Brown, 2008; Prudhomme et al., 2014; Ukkola et al., 2018). For instance, the last two recent assessment report by Intergovernmental Panel Climate Change (AR4 and 5; Christensen et al., 2008; Trenberth et al., 2014) project an increase of drought frequency over subtropical and mid-latitude region while an opposite trend is reported in other studies (Huang et al., 2018; Sheffield et al., 2012; Bonsal et al., 2013). Attributions to the uncertainties in the projections studies point a number of factors such as the difference in the datasets and methods accounting for natural climate variability such as El Nino-Southern Oscillation or warming of tropical Oceans (Giannini et al., 2005). Other studies (e.g., Prudhomme et al., 2014; Ukkola et al., 2018) show that discrepancies in drought evaluation is sourced from the parameterization schemes in the global impact models (GIM) or global climate models (GCMs), such as those used in the fifth Coupled Model Intercomparison Project (CMIP5). Thus, the aforementioned studies point to the need for consideration of multiple models/datasets in drought evaluation so as to account for such unforeseen uncertainties. On the other hand, Burke and Brown (2008) suggest that the selection of drought indices is important source of uncertainties in impact studies and thus recommends utilization of appropriate and most widely robust indices to be employed while assessing drought over a particular domain.

African region, regarded as drought “hotspot” continues to suffer adverse impacts of drought as a result of reduced precipitation (Nicholson, 2000; Hoerling et al., 2006; Lyon and Dewitt, 2012; Liebmann et al., 2014), increased evapotranspiration due to enhanced radiation (Shem and Dickinson, 2006; Abiodun et al., 2008; Nogherotto et al., 2013), increased surface air temperature (Christy et al., 2009; Collins, 2011; Omondi et al., 2014; Camberlin, 2017), warming of the sea surface temperature as result of increased emissions of GHGs (Richard et al., 2001; Hoerling et al., 2006; Manatsa et al., 2014) and changes in the circulation anomalies (Hastenrath et al., 2011; Ogwang et al., 2014). Upward tendencies of observed drought over the continent will lead to potential losses from hazard imposed by a drought event (Touma et al., 2015; Carrão et al., 2018). Recent studies on future drought risk assessment over Africa reveal a dire situation of projected increase in drought risk across the continent with central African countries and North Africa exhibiting aggravating drought hazard (Ahmadalipour et al., 2019). Understanding future evolution of drought scenario across localized domains over the region thus, remains an imperative process in bid to adapt tailor suit innovative solutions to drought risks and their impacts.

Over East Africa (EA), numerous studies have revealed varying trends at historical perspective with some studies showing an increase in severity and frequency of drought (Hulme, 1992; Dai, 2011a; Lyon and Dewitt, 2012; Ayugi et al. 2020). However, future projections point to a varying patterns of drought tendencies, with some studies reporting an increase (Dai, 2011b, 2013; Gidey et al., 2018; Reliefweb, 2019; Haile et al., 2020), while others project an increase of wetting patterns (Shongwe et al., 2011; Williams and Funk, 2011; Maidment et al., 2015). Such uncertainties in projections reveal need for more studies to validate the existing literatures or highlight new tendencies for accurate planning (Kent et al., 2015).

At a local domain such as Kenya, a number of climate related studies conducted have mostly focused on examining historical tendencies with few or no studies at present highlighting the future projections of drought evolutions, either for meteorological, hydrological or agricultural. Few existing studies have focused on projections of either precipitations (Yang et al., 2015; Tierney et al., 2015; Ongoma et al., 2018a) or temperature (Intergovernmental Panel on Climate Change, 2018; Engelbrecht et al., 2015; Dike et al., 2015). Other impact studies have analyzed extreme events based on indices defined by Expert Team on Climate Change Detection and Indices (ETCCDI) and revealed an increasing trend in monthly maximum and minimum vales of daily minimum temperature over large parts of the study domain towards end of the century (Gebrechorkos et al., 2018; Ongoma et al., 2018b).

Droughts continue to persist with devastating impacts on economy, energy and infrastructure, health, land use, society, and water resources. For instance, the economy of the Kenya is based on rain-fed agriculture supporting 80% of food supplies and employment of the 75% of the populations (World Bank, 2012). The observed reduction in seasonal rainfall is likely to impact on future projections of drought. The projections of future climate remain a debate since existing studies have highlighted a contradictory projection, creating a state of confusion on the likelihood of related impact studies on the same (Rowell et al., 2015). Thus, more studies on future projections of precipitation and related impacts remain of great importance. The latest report by global climate risk index 2020 (Eckstein et al., 2020), further paints a worrying situation, with Kenya being classified as 7th most affected and vulnerable country globally to the occurrence of extreme events. To address the gaps, this study seeks to address the existing gap by examining the possible future state of climate based on high resolution biased corrected climate model datasets, sourced from RCA4. In addition, the study will examine the possible projections of drought scenarios based on widely accepted indicator of SPI. A number of studies utilized the aforementioned index in drought analysis across various domains (Dutra et al., 2013; Spinoni et al., 2014; Gidey et al., 2018). However, it should be noted that this index tends to underestimate influence of global warming on drought due to its inability to account for influence of potential evapotranspiration (PET) (Nguvava et al., 2019; Naik and Abiodun, 2020; Spinoni et al., 2020). Due to lack of access to minimum and maximum temperature datasets from the modelling centre, that are prerequisite for accounting for PET, the study utilized SPI that require precipitation data only to compute the drought anomalies. This study is a first step to highlight a glimpse of future projected drought trends over Kenya using high-resolution datasets of RCA4 processed by Coordinated Regional Climate Downscaling framework CORDEX-Africa).

The remaining section of this study is organized as follows: Section 2 describes the data, methods and more description of the study area while Section 3 gives a robust account of findings and discussions of the study. Conclusion and further recommendations are stated in Section 4.

2. Study area, data and methods

2.1. Study area

The focus of this study is over Kenya, located in East Africa along longitude 34° *E*- 42° E and latitude 5° S - 5° N (Fig. 1). Neighboring countries are as follows: Uganda to the west, Tanzania along the south, Ethiopia on the north and Somalia on the east side. The celestial equator crosses the country in the middle placing half to the southern hemisphere and other half in the northern hemisphere. The country has massive and diverse geographical features. The Great Rift Valley passes across the country from Ethiopia to the North through to Tanzania in the south. The western side of the study area has higher elevation while plains characterize the eastern side. Meanwhile, the eastern Kenya have large expanse of drylands with aridity index ranging from $0.05 \leq AI \leq 0.2$ in some regions to $0.2 \leq AI \leq 0.5$ in other areas (Huang et al., 2016). Consequently, the region is considered as a dry climate anomaly in an otherwise wet equatorial belt (Camberlin, 2018).

Climatology of rainfall is featured by bimodal pattern with seasonal

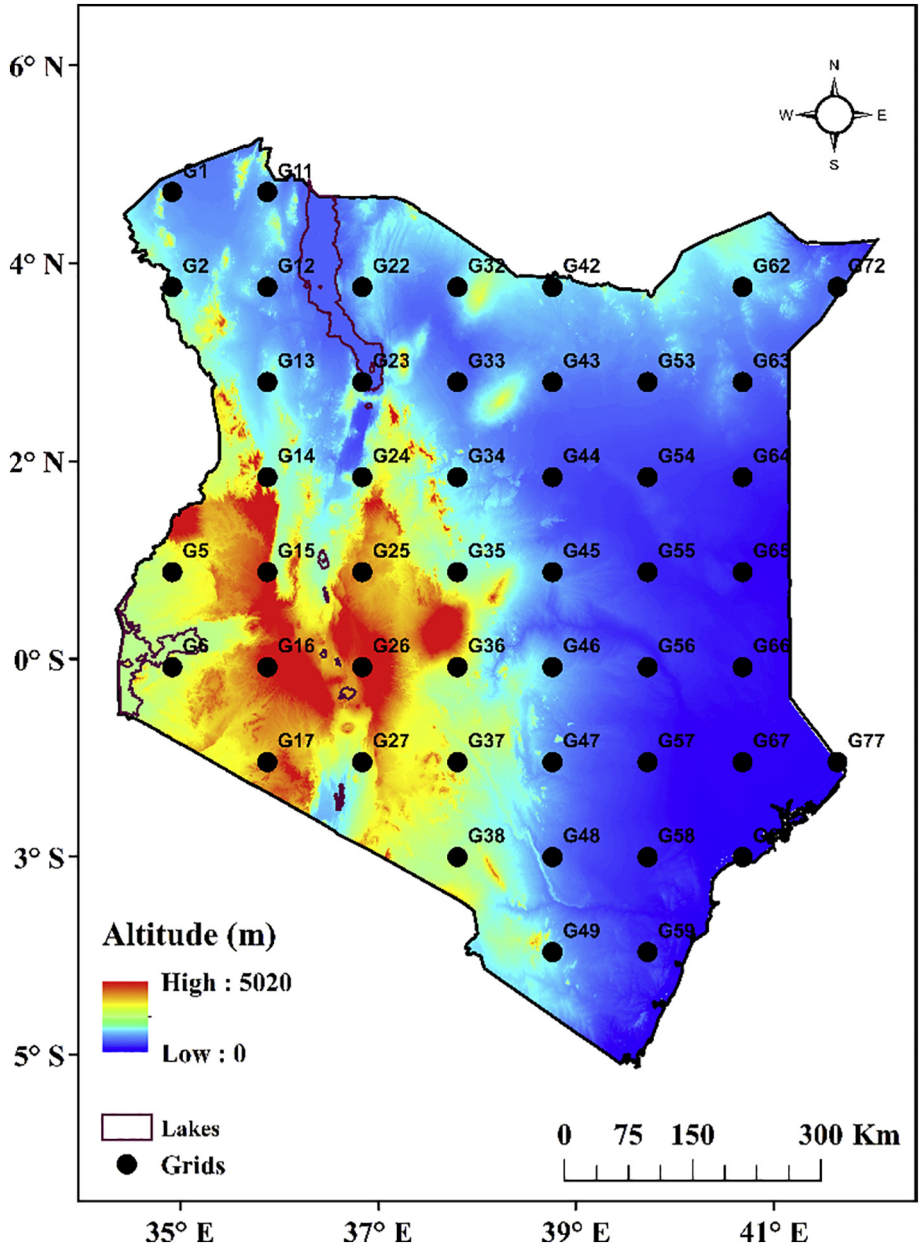

Fig. 1. The study area [34°E–42°E and 5°S–5°N] with topographical elevation (m) in blue/red color. (For interpretation of the references to color in this figure legend, the reader is referred to the web version of this article.)

rains experienced from the month of March to May (MAM) and second regime beginning from October to November (OND). A number of studies (Philippon et al., 2002; Hastenrath et al., 2004), note that the second regime rainfall is characterized by more coherency in spatial distribution as compared to local wet MAM season which is regarded as "long rains" over the study locale. These seasons are associated with maximum solar heating driven by the oscillating migration of the rain belt along the Inter-Tropical Convergence Zone (ITCZ) (Camberlin and Okoola, 2003; Yang et al., 2014). The ITCZ drives a remarkable influence in the distribution and patterns of rainfall and temperature fluctuations over the study area (Nicholson, 2008; Ogwang et al., 2014; Maidment et al., 2015). The country is generally characterized by warm temperature throughout the year, with slight variations from one season to another, thus defined as a tropical savanna climate (Aw) (Peel et al., 2007). Mean annual temperature over the study region ranges between 19 and 30 °C. The warmest months are January and February (JF), followed by MAM season, while June–September (JJAS) record the lowest temperatures (King'uyu et al., 2000; Schreck and Semazzi, 2004; Ongoma et al., 2017; Kerandi et al., 2018). The cold zone is generally in the areas at high elevation, on either side of the Rift Valley. In support of the elevation effect on temperature, low temperatures are observed near the central and Rift Valley regions. The eastern and northwestern parts of the country record the highest temperatures since the areas are mainly Arid and Semi-Arid Lands (ASAL); characterized by low rainfall. The northeasterly winds prevail during the JF and JJAS seasons while the south easterlies are dominant during MAM and OND (Hastenrath et al., 2011).

Numerous studies have been conducted to ascertain historical drought variabilities, trends and the respective impacts on agriculture, economy, water resources and environment over the study region (Zargar et al., 2011; Changwony et al., 2017; Frank et al., 2017; Karanja et al., 2017; Mutsotso et al., 2018; Wambua et al., 2018; Polong et al., 2019). These researchers have reported varying features of drought variation and trends over the study region. Ayugi et al. (2020b) detailed

more information regarding an in-depth analysis of recent trends, frequencies, intensity and duration of drought patterns over the study domain using robust index of Standardized Precipitation Evapotranspiration (SPEI).

2.2. Data

This study utilizes MME of five selected RCMs. The models are as follows: Model for Interdisciplinary Research on Climate (MIROC5), Commonwealth Scientific and Industrial Research Organization (CSIRO), Institute Pierre Simon Laplace Model CM5A-MR (IPSL-CM5A-MR), Max Planck Institute Earth System Model at base resolution (MPI-ESM-LR) and European community Earth-System (EC-EARTH). The listed RCMs simulations outputs are derived from the dynamical downscaling of CMIP5 GCMs using RCA4, originally developed by the Swedish Meteorological and Hydrological Institute (SMHI) under the CORDEX initiative (Samuelsson et al., 2012). The RCA4 is a product of major enhancement on RCA3 based on model experimental design. Unden et al. (2002) and Strandberg et al. (2015) detailed more information regarding the physics of RCA4 model. The RCA4 simulations outputs are available on CORDEX-Africa domain have spatial resolution at grid increment of 0.44° × 0.44° (~50 km × 50 km) and temporal coverage ranging from 1951 to 2005 for historical runs and projections from 2006 to 2100. Table 1 present the details of models that were used to derive the ensemble as used in the present study. Ayugi et al. (2020b) evaluated the performance of the listed RCMs and noted a better performance over the study domain in simulating precipitation. Similar performance was observed over larger domain of Greater Horn of Africa (Endris et al., 2013; Kisembe et al., 2018). Further, the models were bias corrected based on a quantile mapping bias corrected algorithm in order to minimize possible bias for accurate projections. Ayugi et al. (2020c) outlines more information regarding the techniques for quantile mapping bias correction that was employed to reduce the biases in the models. Findings demonstrated that using QMBC on outputs from RCA4 is an important intermediate step to improve climate data before performing any regional impact analysis. For instance, the results show that most of the models exhibit reasonable improvement after corrections at seasonal and annual timescales. Specifically, the EC-EARTH and CSIRO models depict remarkable improvement as compared to other models. On the contrary, the IPSL-CM5A-MR model shows little improvement across the rainfall seasons MAM and OND. (See Table 2.)

2.3. Methods

Analysis for the MME was carried out under different RCPs; RCP4.5 (midrange) and RCP8.5 (high) emissions scenarios (Moss et al., 2010). Three-time slice 30-year period, near-future (2010–2039), mid-term (2040–2069) and late century (2070–2100), was considered for investigation of drought and flood events, relative to the reference period (1971–2000). The techniques applied are described as follows:

2.3.1. Theil-Sen slope

The present study employed Theil-Sen Slope technique to appraise the long-term trend in the precipitation anomaly data over the study region. This is non-parametric method that is employed to evaluate the magnitude of the slope of the linear trend in a sample of "n" pairs of data (Sen, 1968; Sun et al., 2011). This method is considered effective due to its robust features of outliers in the datasets. It is not affected by any extreme distributions and does not entail any normal distribution of the residuals. It has been widely employed to study the linear trends of hydro climatic variables (e.g Ongoma et al., 2017; Wang et al., 2018). Mathematic expression of equation for Theil-Sen slope, X*i,* of a time series can be calculated as.

$$Xi = \frac{qi - qj}{j - k} \text{ for } I = 1, 2, 3...n \quad (1)$$

where q_i and q_j represent the data value at time j and k (j > k), respectively.

2.3.2. Modified Mann-Kendall test

Commonly utilized non-parametric rank-based modified Mann-Kendall (m-MK) test (Mann, 1945; Kendall, 1975; Sneyers, 1990; Hamed and Rao, 1998), suitable in detecting trends in any paired data is employed in the present study. The advantage of m-MK test is its capability of incorporate missing values in any time series and also due to the fact that it employs relative magnitudes rather than numerical values that allows 'trace' or 'below' detection data (Hirsch et al., 1993; Zhai and Feng, 2009). Numerous hydro-climate studies across various have employed this technique for trend analysis (Ongoma et al., 2017; Ayugi and Tan, 2019).

2.3.3. Standardized precipitation index (SPI)

The SPI is a tool developed to quantify drought at a given time interval (temporal resolution) for precipitation distribution from historical data. This tool can also be used to monitor periods of anomalously wet/dry events. According to McKee et al. (1993), SPI calculation is based on the long-term precipitation taken for the required period. The computation of the SPI involves fitting a gamma probability density function to a given frequency distribution of rainfall tools for station. The alpha and beta parameters of the gamma distribution are estimated for each timescale of interest (i.e 1, 3, 6 and 12 months) and for each month of the year. The gamma distribution is defined by its probability density function:

$$g(x) = \frac{1}{\beta^{\alpha}\tau(\alpha)} x^{\alpha-1} e^{-\frac{x}{\beta}}, \; x \geq 0 \quad (2)$$

where α and β are shape and scale parameters, x is the rainfall amount and $\tau(\alpha)$ is the gamma function. Maximum likelihood solutions are used to estimate $\alpha$and β.The resulting parameters are then used to find the cumulative probability of observed rainfall event for a given month and timescale. The cumulative probability, after its computation, is transformed to the standard normal random variable $z$with a mean equal to 0 and the variance of 1, which is the value of the SPI.

The standardization ensures that the SPI gives uniform measure for wetness and dryness in different climate regimes or under seasonal dependence. Drought severity is defined as the cumulative sum of the monthly SPI values considering SPI values above/under a certain threshold. The threshold considered in the present study is similar to that of SPEI of greater/less than +1.0 or − 1.0, which represents the limit of wetness or dryness. A number of studies have employed SPI in

Table 1
The description of the global climate models (GCMs) dynamically downscaled by Rossby Centre Regional Climate Model (RCA4) CORDEX.

Institute	Native horizontal grid increment	Abbreviated Name
1. Consortium of European Research Institutions and Researchers, Netherlands	1.125° × 1.125°	ICHEC-EC-EARTH
2. Institute Pierre Simon Laplace, France	3.75° × ~1.895°	IPSL-IPSL-CM5A-MR
3. National Institute for Environmental Studies, and Japan Agency for Marine-Earth Science and Technology (MIROC), Japan	~1.4° × 1.4°	MIROC-MIROC5
4. Commonwealth Scientific and Industrial Research Organization (Australia)	~1.875° × 1.875°	CSIRO-Mk3.6.0
5. Max Planck Institute for Meteorology (Germany)	~1.875° × 1.875°	MPI-M-MPI-ESM-LR

Table 2
the duration, severity, and intensity occurrence of drought for SPI 3 and 12- timescale for RCP 4.5 and RCP8.5 during near-future [2010–2039], mid-term [2040–2069], and late-century [2070–2100] over Kenya.

SPI	Duration			Severity			Intensity		
RCP4.5	2010–2039	2040–2069	2070–2099	2010–2039	2040–2069	2070–2099	2010–2039	2040–2069	2070–2099
SPI-3	58	53	53	−87.57	−74.33	−71.70	−1.50	−1.40	−1.41
SPI-12	44	53	49	−77.21	−79.04	−69.76	−1.75	−1.50	−1.42
RCP8.5	Duration			Severity			Intensity		
SPI-3	53	53	51	−78.59	−81.56	−75.41	−1.48	−1.53	−1.50
SPI-12	64	57	53	−86.17	−87.94	−71.71	−1.34	−1.54	−1.35

drought assessment across different parts of the study region (Manatsa et al., 2010; Wambua et al., 2018; Changwony et al., 2017).

In this study, the study duration was sub-divided into three time slices, each with cumulative period of month/years (360/30); i.e., near future (2010–2039); mid-century (2040–2069); and late-century (2070–2100). The aim of sub-dividing the study duration in three different time slices is to test if there may be a likelihood of noteworthy deviations in the drought conditions between different periods. This approach has been implemented in a similar study across various domains (Ionita et al., 2016; Ahmadalipour et al., 2017b; Huang et al., 2018).

The present study considered the duration of dryness situation by the length of time (months) that the drought index is consecutively above or below a truncation value (i.e SPI ≤ -1.00). The SPI values were calculated in two-time scales namely, the SPI-3 and SPI -12 (McKee et al., 1993) for three different categories: *moderate* ($-1.49 <$ SPI < -1.00), *severe* ($-1.99 <$ SPI < -1.50) and *extreme* (SPI ≤ -2.00). These values for the SPI define the feature of drought events in terms intensity, severity and frequency of extreme events define drought episodes. Similar method has been employed in other studies (Polong et al., 2019; Ayugi et al., 2020a).

Shorter time scales of 3 months are employed to detect soil moisture anomalies while longer time scales determine hydrologic drought (Balint et al., 2011). For instance, the months of March to May (MAM) over the study area represent the growing season, supporting 80% of agricultural activities. In addition, soil moisture is fully utilized during this season, hence the deficit is associated with drought condition (e.g Hayes et al., 1999; Manatsa et al., 2010). Significant percentage of total annual rainfall is experienced during the season covering entire study location, and as such, water availability for land cover vegetation is primarily influenced with seasonal rainfall. The analysis was conducted for different representative concentrative pathways, i.e. RCP 4.5 and RCP 8.5 (Riahi et al., 2011).

The advantage of the SPI approach is the spatiality consistent. It gives the comparisons between different locations in different climates (climatic sub-regions) regardless of the fact that they may have different normal rainfall (Hayes et al., 1999). In addition, it is adaptable to any other climatic variable apart from precipitation (Vicente-Serrano and López-Moreno, 2005).

Further, this study defined the severity, intensity, and frequency for dry/wet event over the study domain as given in Eqs. (3)–(5);

i) Severity is the cumulative sum of the index value based on the duration extent (Eq. (3));

$$S = \sum_{i=1}^{Duration} Index \tag{3}$$

ii) Intensity of an event is the severity divided by the duration (Eq. (4)). Events that have shorter duration and higher severity will have large intensities.

$$I = \frac{Severity}{Duration} \tag{4}$$

iii) Frequency of occurrence (F_s) is defined in the Eq. (5);

$$F_s = \frac{n_s}{N_s} x\ 100\% \tag{5}$$

where n_s is the number of drought events (SPEI < -1.0), N_2 is the total of the months for the study period, and s is a grid cell.

In order to demonstrate the regions most affected by the occurrence of drought events, also referred as "hotspots" zone, the SPI analysis was conducted at pixel-wise zone. For instance, all datasets were extracted from 59 grid cells within the study domain (Fig. 1). This was derived from re-gridding of datasets using bilinear interpolation to 1° x 1° spatial resolution in bid to achieve uniform grids. The dominance of the dry cases was examined on the percentage of frequency of each incidence with reference to the total number of months. This approach was successfully employed in a recent study of drought evaluation along the major water basin in Kenya (Polong et al., 2019) and overall study domain (Ayugi et al., 2020a). The intention of employing this approach was to categorize regions that frequently experience concurrence of extreme and severe climatic cases at corresponding periods.

3. Results and discussions

3.1. Projected changes in rainfall

Drought occurrence is entropic natural event that is mainly influenced from the changes in climatic variables, namely precipitation and temperature (Sheffield and Eric, 2008). Deviations in drought scenarios are mainly determined by precipitation anomalies with acute deficit resulting to severe or extreme drought situation (Dai et al., 2018). It is thus important to examine projected patterns of rainfall event in order to understand the changes in drought and pluvial occurrences over a particular study domain. In this study, the changes in annual and seasonal precipitation over Kenya are examined in order to associate with changes in drought occurrence. Various statistical models are employed in assessing the climatic variable employed in this study. Fig. 2 presents the probability function distribution (PDFs) for annual and seasonal rainfall changes for baseline and for projections based on RCP4.5 and RCP8.5 scenarios. This function is useful in explaining the likelihood of an outcome for stochastic variable based on deviations from the mean value. In this study, the PDFs for projections were conducted under three time slices, namely; near future (2010–2039), mid-century (2040–2069) and towards the end of the century (2070–2100). Results demonstrate positive shift, indicating an increase in projected rainfall change during all the three timescales. Most of the changes in variance are statistically insignificant at 95% confidence interval, except for RCP4.5 scenario during mid-term (2040–2069) for OND.

The projections under RCP4.5 scenario during three time slices (Fig. 2a) shows less deviations of the models from the baseline during near-future and mid-century, indicating dry scenarios during MAM season. However, a positive shift is noted towards the end of the

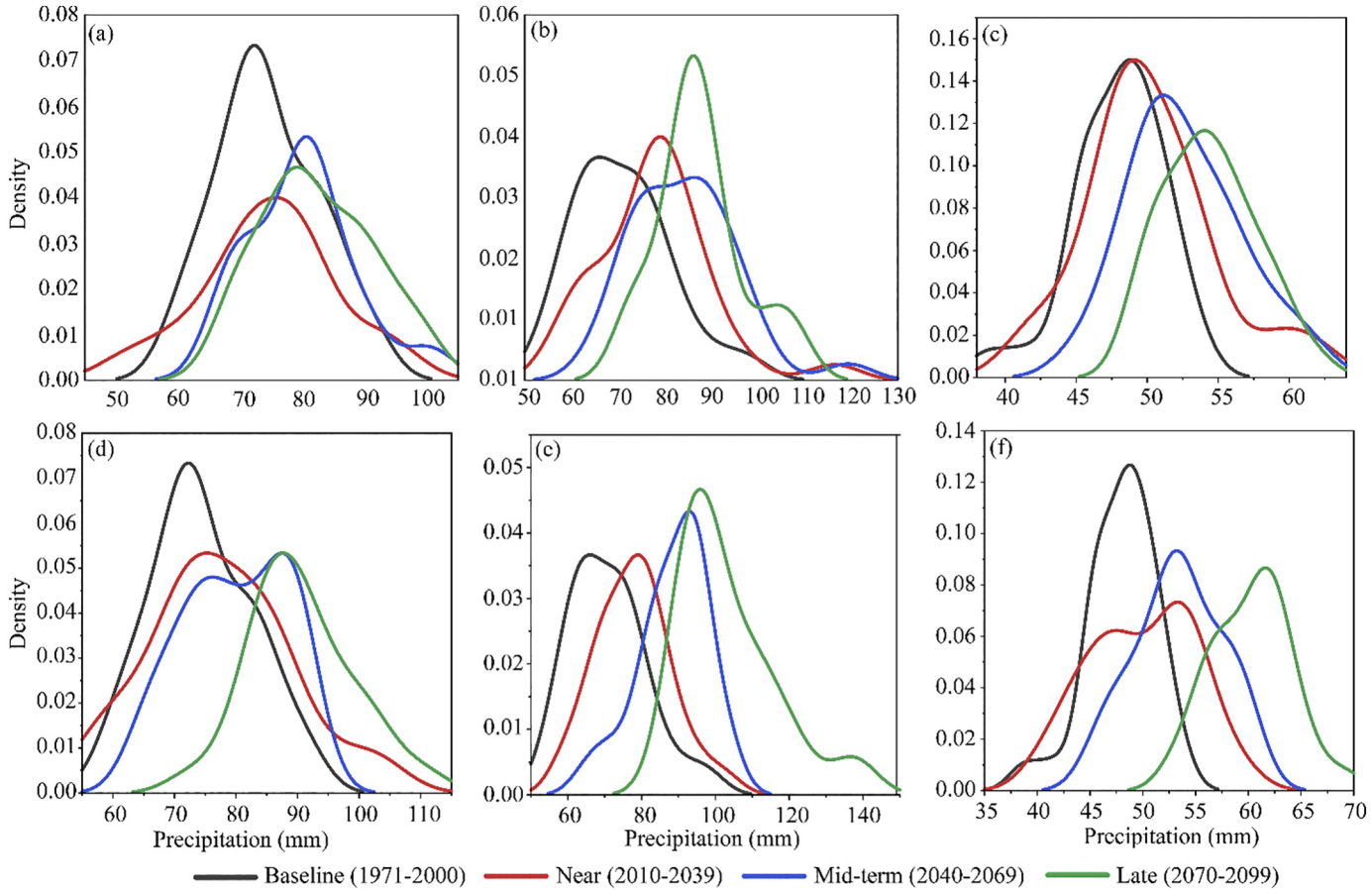

Fig. 2. Probability density functions (PDFs) for seasonal, (a) MAM, (b) OND, and (c) Annual under RCP 4.5 scenarios while (d) MAM, (e) OND, and (f) show annual precipitation distribution under RCP 8.5 over Kenya.

century. During the OND season (Fig. 2b), the model shows large shift, indicating increase in rainfall amount as compared to historical baseline period (1970–2000). This shows that the study area is likely to experience a shift in seasons, with historically known 'long-rainy season' of MAM, shifting towards OND, which has been historically referred as 'short rainy-season'. Previous studies note that OND tends to depict stronger inter-annual variability, stronger spatial lucidity of rainfall anomalies across most region, and substantial association with ENSO and Indian Ocean Dipole (IOD) (eg. Indeje et al., 2000; Nicholson and Kim, 1997; Endris et al., 2019).

Annual PDF (Fig. 2c) show a similar patterns as seasonal rainfall event with positive shift in all the three time slice experienced. Compared to MAM season, the deviation received during annual show large differences between baseline period and the projected scenarios. This shows that the region will become wetter as compared to the historical experience that has been characterized by incidences of drought across the study domain. The findings of this study agree with other existing literature that have reported an increase in rainfall frequency over the study domain (Kent et al., 2015; Maidment et al., 2015; Ongoma et al., 2018a). Zhao and Dai (2017) linked the wetting trend over East Africa region to a robust response of the Indian Ocean ITCZ. However, some studies, i.e. Tierney et al. (2015) based on paleoclimate datasets, project drying patterns, mostly associated with weakening in the Walker Circulation over Indian and Pacific Ocean basins. This confusion scenario of projected rainfall trends is termed as East Africa "climate paradox" and calls for more evaluative studies to ascertain the clear projected patterns (Rowell et al., 2015).

The PDFs for rainfall projections under RCP8.5 scenario (Fig. 2d-f) for MAM, OND and annual show larger deviations as compared to RCP4.5 scenario. For instance, during OND (Fig. 2e), the late-century (2071–2100) will likely to experience substantial intensification in rainfall frequency as compared to other time slices. The strong shift, indicating the increase in rainfall event, despite the projected future warming, agrees with a study of Kent et al. (2015) that reported lack of correlation between uncertainty in global mean temperature and projected end-of-twenty-first-century change in precipitation. On the contrast, the study noted that the uncertainty in regional precipitation over study region is predominantly related to spatial shifts in convection and convergence, associated with processes such as sea surface temperature (SST) patterns and land-sea thermal contrast change. The conclusion of various studies attempts to elucidate the shifts in rainfall projections highlights the complexity of regional rainfall changes which leads to uncertainty on the impact, mainly on extreme events occurrences.

3.2. Projected changes in drought events

Fig. 3-5 depict spatial distribution of projected total moderate, severe, and extreme drought frequencies over different time slices; (a) 2010–2039, (b) 2040–2069, and (c) 2070–2100 relative to the period 1971–2000 for SPI-3 under RCP4.5 scenario while (d-f) under RCP8.5 scenario, with similar time slice as aforementioned pathways. The SPI-12 is presented in the figures (g-l); (g) 2010–2039, (e) 2040–2069, and (f) 2070–2100 for RCP4.5 scenario while (j) 2010–2039, (k) 2040–2069, and (l) 2070–2100 for RCP 8.5 scenario. The analysis for SPI was derived from ensemble of 5 bias corrected RCMs simulations over Kenya. Units for the frequency reflected are based on the number of months/periods in which drought occurrence took place at a particular region.

Analysis of moderate drought duration for SPI-3 under the RCP4.5 scenario for near future (Fig. 3a) shows varying patterns of drought

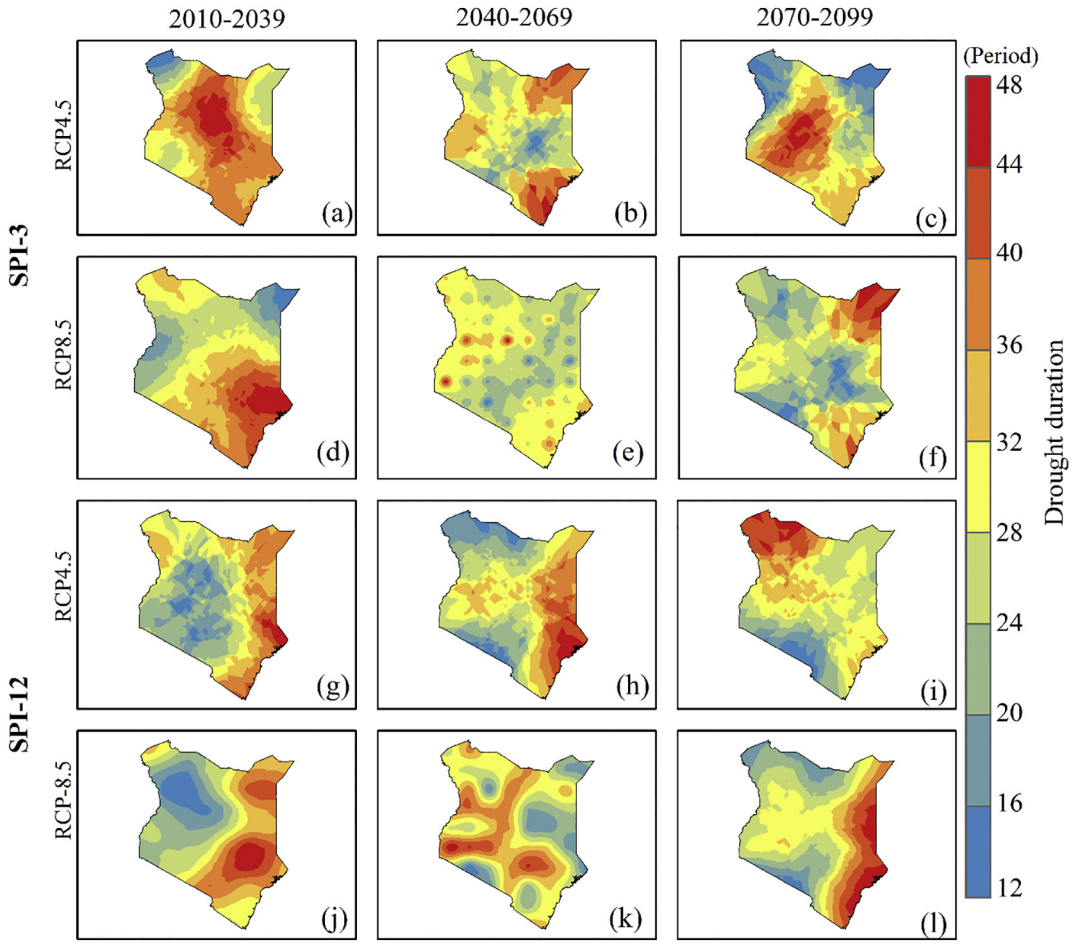

Fig. 3. Spatial distribution of projected *total moderate drought* ($-1.49 < \text{SPI} < -1.00$) duration over different time slice; (a) 2010–2039, (b) 2040–2069, and (c) 2070–2100 relative to the period 1971–2000 for SPI-3 under RCP4.5 while (d-f) for RCP8.5, with similar time slice as aforementioned pathways. The SPI-12 is presented in the figures (g-l) with Figures; (g) 2010–2039, (e) 2040–2069, and (f) 2070–2100 for RCP 4.5 while (j) 2010–2039, (k) 2040–2069, and (l) 2070–2100 for RCP 8.5 derived from ensemble of 5 RCMs simulations over Kenya. Units: number of months/periods.

frequencies with regions along the northeast and southeast, stretching towards coastal belt likely to experience higher number of months affected by moderate drought as compared to other parts of the study area. For instance, moderate droughts show reduction in occurrence towards the mid-century (2040–2069), except in southern belt, and far end northeastern sides that continue to exhibit higher duration of drought occurrence (48/360 months). The locations along eastern sides stretching to the southern belt of the study area are mostly characterized by bare ASALs. Climatic characteristics of such region is predominantly dry with below normal rainfall experienced, leading to increased evapotranspiration which is induced by enhanced radiation, higher wind speed, and vapor pressure deficit, mostly linked to higher temperature and low relative humidity. Interestingly, locations suited along the western sides and northwest will likely to experience fewer months of moderate drought duration. These locations have large water bodies and high elevations coupled with dense vegetations.

During the RCP8.5 scenario for SPI-3 (Fig. 3d-f), the study area will likely to experience homogenous distribution of mild moderate drought during mid-century and further reduction in drought occurrence towards the end of the century (Fig. 3f). This pattern of drought incidences tends to follow the projected trends of precipitation patterns that show significant increase in future under the scenarios over the study domain, most especially under higher emission scenarios (Shongwe et al., 2011; Tierney et al., 2015; Ongoma et al., 2018a). The projected increase in precipitation signifies of more pluvial scenarios as compared to drought incidences with risk such as flooding which will ultimately impact on disaster management programs due to infrastructural loss. New emerging challenges will arise due to the coupling scenarios where the projected surface temperature anomalies show positive trajectory of across the globe and over the study region (Ongoma et al., 2018a). The study area is likely to encounter serious problems associated with health as a result of vector borne disease and other pestilences.

The above-mentioned studies, further state that the increment in precipitation amount, will be more pronounced during the period OND season as compared to the MAM season which also is in harmony with the findings of the present study as demonstrated in Fig. 2. Numerous studies (i.e., Saji et al., 1999; Endris et al., 2016; Endris et al., 2019) have pointed the influence of Indian and Pacific Ocean with important changes in the strength of teleconnections, mostly related to ENSO and IOD. For instance, Endris et al. (2019) show a dipole future changes in precipitation, with a stronger ENSO/IOD related to rainfall anomaly over most eastern parts of the study area, but a weaker ENSO/IOD signal over the southern parts of the study area. The projected changes in rainfall that are linked with mean changes in SST and associated with Walker Circulations, with impacts varying across the spatial scale over the study locale is reflected during the SPI-12 under both RCP4.5 and RCP8.5 scenarios (Fig. 3g-l). The present analysis shows that most spatial patterns continue to exhibit the hotspots located along the southeastern regions characterized by coastal planes while western and central are showing few months of drought duration. The regions located along highland plateau featured by the presence of raised table

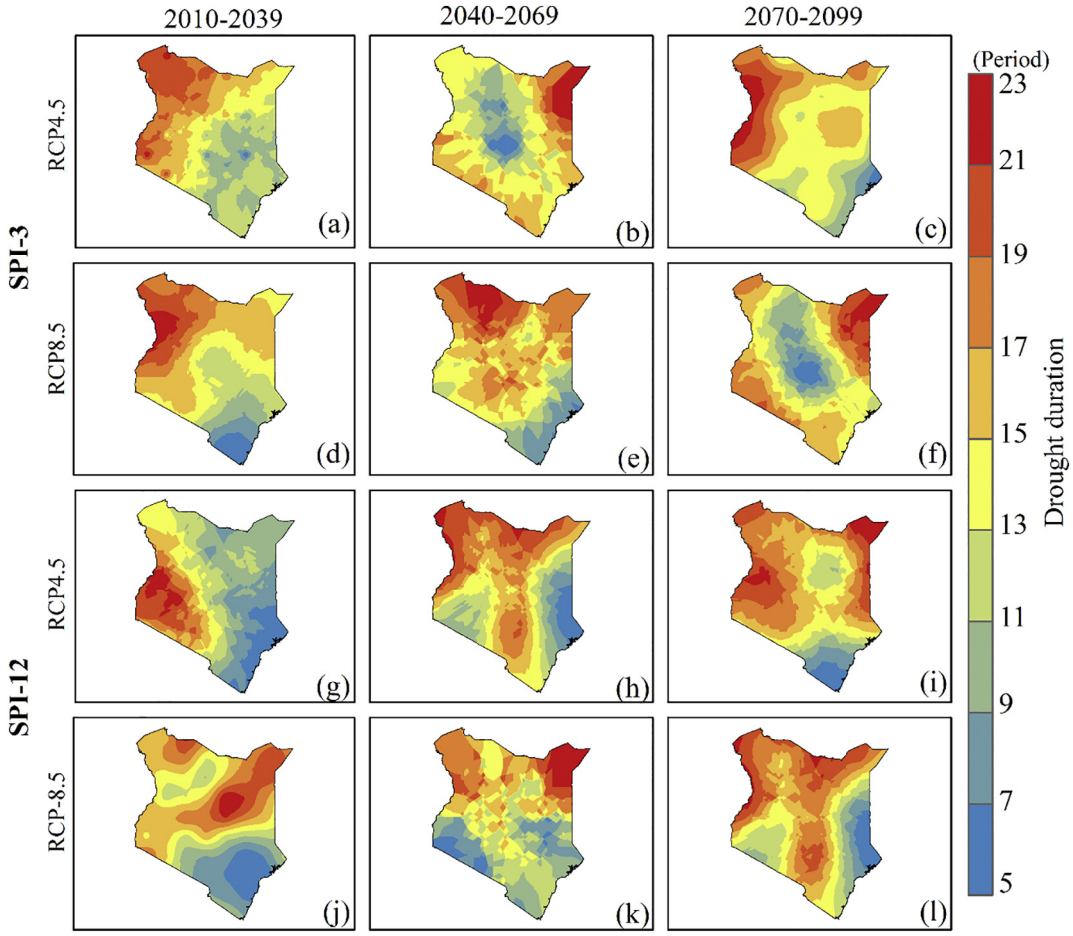

Fig. 4. Same as Fig. 3 but for *total severe drought* duration ($-1.99 < SPI < -1.50$).

land above sea level and large water bodies with humid climate will likely to experience few occurrences of drought events along such regions. Recent study (Haile et al., 2020) established that the wetting/drying patterns are directly linked to the widely known concept of 'dry gets drier and wet gets wetter' paradigm. This pattern is mainly associated with the P and PET which are main variables in the calculation of the drought index. These are further associated with the water balance (P-PET) estimations where humid regions hold wet with positive P-PET value while arid regions result in deficit/negative P-PET.

In terms of severe drought (Fig. 4), the period 2010–2039 is characterized by fewer months with which the study area is likely to experience drought occurrence as compared to moderate drought. The highest duration during this category has a total of 23 months (out of 360 months) and least is < 5 months over the study duration. Particularly, for the SPI-3 (Fig. 4a-f), the study locale shows varying patterns of drought hotspots regions, mostly over the northwest and northeast. The central regions show relatively low drought events as compared to other parts of the study area. The late century (2070–2100) shows an increment in severe drought duration covering almost the entire country with substantial scenarios manifesting for SPI-12 under business as usual scenarios (Fig. 4i). Overall, the study area shows that most parts will likely to experience severe drought during SPI-3 as compared to SPI-12 in all the three-time slice.

In Fig. 5, the hotspots regarding the extreme drought are depicted for SPI-3 (Fig. 5a-f), and SPI-12 (Fig. 5g-l) under two RCP4.5/8.5 scenarios. Analysis for SPI-3 under RCP4.5 scenario (Fig. 5a-c) shows substantial period in which the region will experience drought incidences, mostly over the western sides (2010–2039) and northwestern (2040–2069). However, reduction in drought occurrence is likely to be experienced across western and southern regions towards the end of the century under stabilization control scenario (Fig. 5c). During the RCP 8.5 scenario (Fig. 3d-f), the abnormal occurrence of drought events is depicted along northeast section of the country. The economic activity of the community residing around this area will likely to be affected since their main economic activity is solely relying on pastoralist livelihood. A recent baseline survey (Mutundu et al., 2013), conducted in bid to establish the interventions in upgrading animal health and production in the wake of increased severe drought occurrence prevailing currently and projected to increase, revealed fragile situation with lack of enough infrastructure to enable community cope with adverse effects of droughts. This calls for more intervention measures so as to enable affected members of the society cope adequately with expected drought incidence in the near and mid-century time slice period. The plots for SPI-12 in the period under RCP4.5/8.5 scenario (Fig. 5j-l) depict a strong reduction in the amount of drought that the country is likely to experience. Interestingly, the western sides of the study area show higher duration of drought occurrence and the southwestern as compared to other parts of the region.

3.3. Projected changes in drought intensity, frequency and severity

Fig. 6 provides an overview of projected changes in drought frequency and severity analysis for SPI 3 timescale under (a) RCP4.5 and (b) RCP8.5 scenarios during three time slices namely; near future (2010–2039), mid-term (2040–2069), and late-century (2070–2100) over Kenya. Fig. 6(c) and 6(d) show the results for SPI 12 timescale under RCP4.5 and RCP8.5 scenarios respectively. The evaluation of drought events was conducted based on SPI classifications for

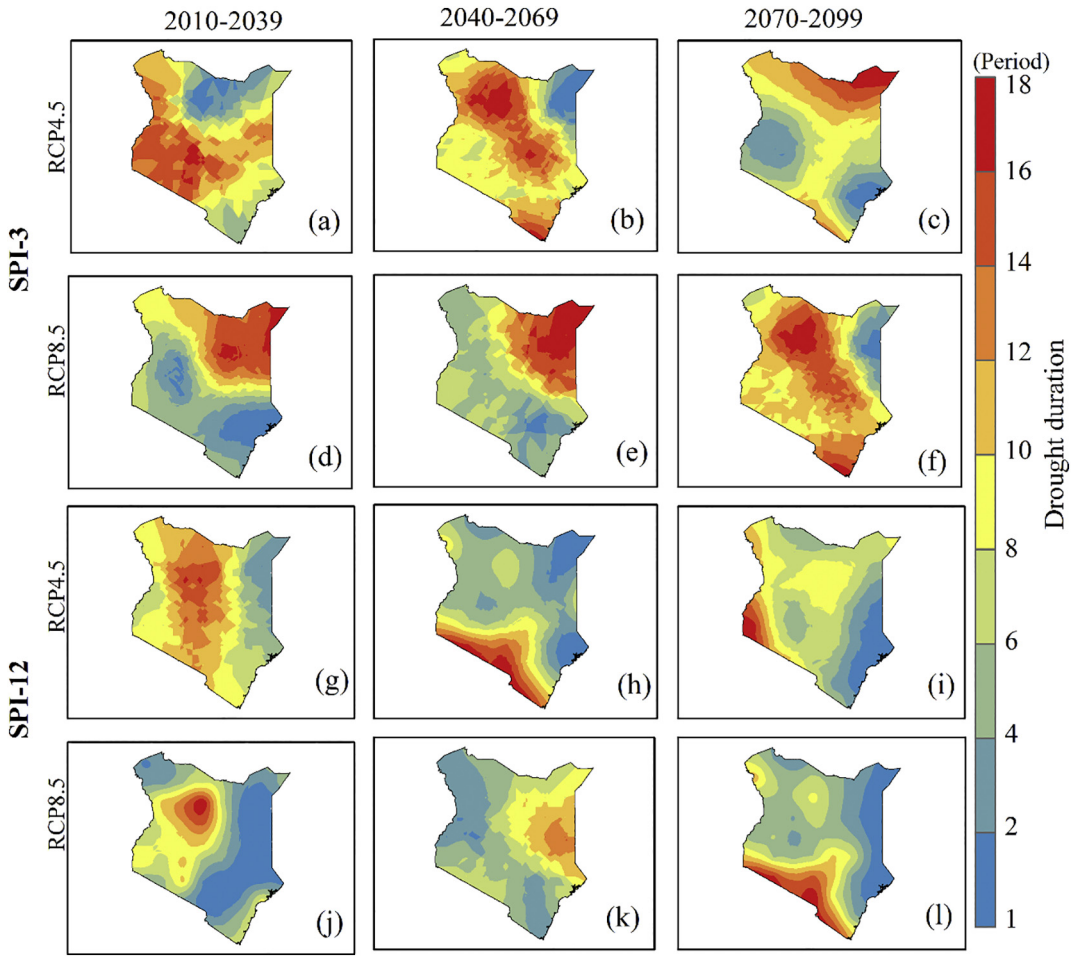

Fig. 5. Same as Fig. 3 but for total extreme drought duration (SPI ≤ −2).

moderate, severe and extreme frequencies (Vicente-Serrano et al., 2010; Beguería et al., 2014). From the SPI-3 results for RCP 4.5 scenario during the first time slice (Fig. 6a), it can be seen that the study domain will likely to experience intensification of more severe to extreme incidences towards the end of the near-century period. During mid-century projections for SPI-3 (Fig. 6a), the study domain will experience more of severe and extreme drought scenario as compared to moderate incidences. However, mid-century and late century projections show that the study area is likely to experience sharp reduction in severe and extreme occurrence to more of moderate drought frequency. Late-century drought projections under medium stabilization without shoot show occurrence of moderate to severe events and likely occurrence of high intense occurrence of extreme event. The causes for this outrageous occurrence of extreme drought are still unknown and likely to elicit for further studies. Analysis for drought possible scenario for SPI-3 under RCP8.5 is shown in Fig. 6b. Similar to medium-term scenario analysis, three-time slice representing near future, mid-term, and end-century were considered. The results show intensification of severe and extreme in the whole time slice while a reduction of moderate drought across the study period. The study area is likely to experience extreme drought frequency during the early century of the study period (Fig. 6d). On the other hand, the mid-century depicts continued occurrence of extreme and severe. The observed changes in drought characteristic during mid-century indicate the intensity phenomenon at −1.53, with the severity occurrence recording a stronger event of −81.56 over the duration of 53 months (Table 1). It is apparent from results presented that SPI-3 exhibit greater temporal frequencies of the occurrence for wet and dry cases during the study duration. The last time slice for 2070–2100 for SPI-3 under RCP8.5 (Fig. 6b) depicts sustained incidences of extreme drought occurrence.

Fig. 6c and d demonstrate the results of meteorological drought events for SPI-12 under RCP 4.5 (Fig. 6c) and RCP8.5 scenarios (Fig. 6d) during the near future (2010–2039), mid-term (2040–2069), and late-century (2070–2100). The reduction in drought incidences during mid-century under RCP8.5 scenario (Fig. 6d) concur with precipitation projections that are reported to increase during the mid of the century (Shongwe et al., 2011; Christensen et al., 2013; Ongoma et al., 2018a). Similar results were equally observed in the present study that demonstrated a recovery of MAM seasonal rainfall and significant positive deviation during OND season for the period 2040–2069 across the study domain (Fig. 2). Recent studies on inter-annual precipitation changes have showed robust association of rainfall and SST anomalies, namely Indian and Pacific Oceans (Behera et al., 2005; Shongwe et al., 2011; Christensen et al., 2013). The conclusion of these studies demonstrates that long-term greenhouse gas forced SST pattern variations in over the study domain could contribute to precipitation change, thereby impacting on drought or flood respectively. The drought severity incidences for further analysis, which was derived as sum of the index value based on duration extent are presented in Table 1. The result for SPI-12 under RCP4.5 scenario for near-future shows an overall severe drought occurrence over the study location with observed intensity of −1.75 and cumulative frequency of 44 months during the study period (Table 1).

Comparison of the two indices shows that SPI-3 is characterized by moderate drought occurrence while long-term drought (SPI-12) shows reduction in the extreme events over the study area. This agrees with other future drought projections over broader region of East Africa. For instance, a recent study over Ethiopia (Abrha and Hagos, 2019),

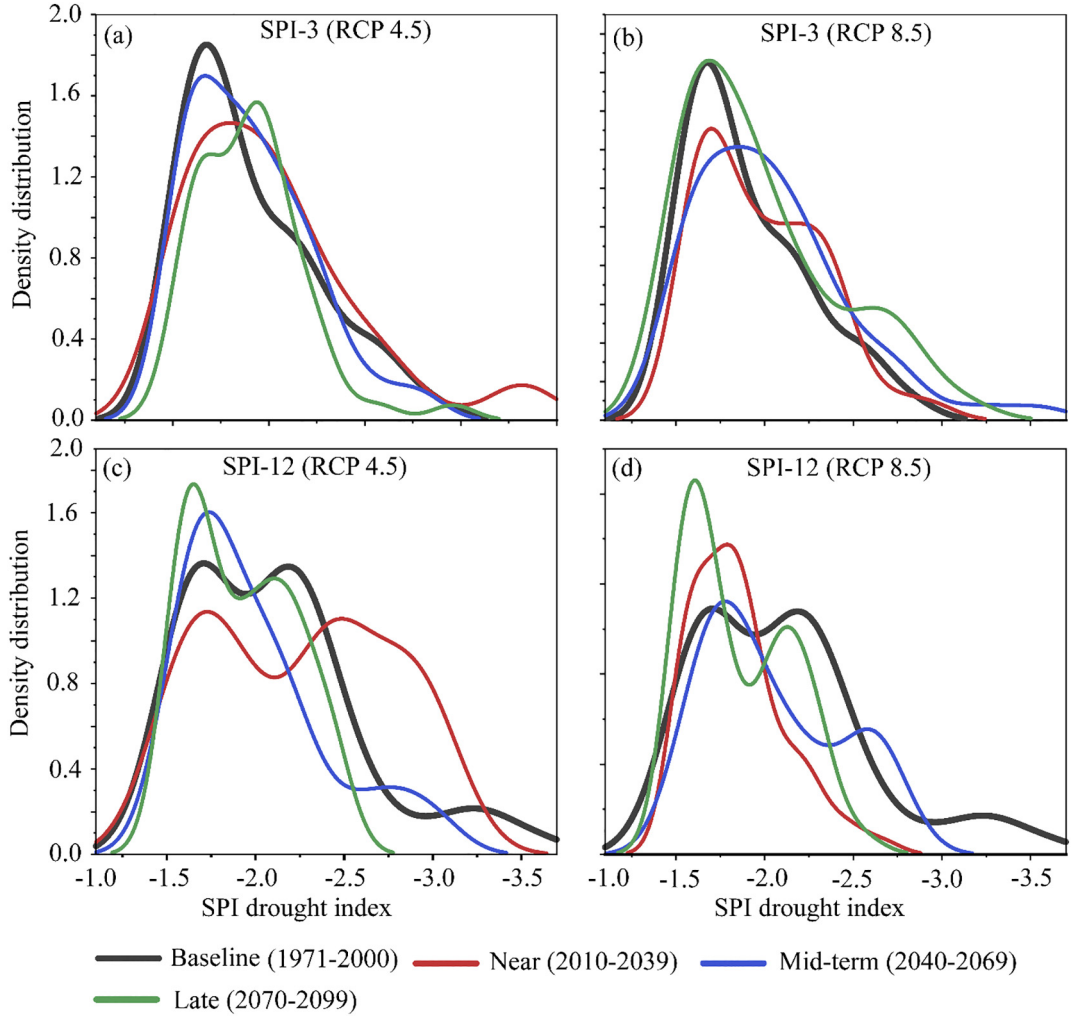

Fig. 6. Evolution of meteorological drought events in 30-year intervals for SPI 3 (12)- timescale for RCP 4.5 (a) (c) and RCP8.5 (b) (d) during near-future [2010–2039], mid-term [2040–2069], and late-century [2070–2100].

reported an increase in moderate dry conditions at 16.7% and slight increase of extreme occurrences at 6.7%. This study used an ensemble of seven drought indices, namely; SPI, percent normal, EDI, *Z*-score RAI, Modified China Z-score, and RDI using meteorological drought monitoring and DricC software. However, some regions have demonstrated an increase in severe and extreme drought scenarios, which is contrary to the projected trends over East Africa. To illustrate, drought projections over South African region based on SPEI and SPI show that simulations project a robust increase in the magnitude of drought intensity and frequency, which is likely to significantly increase under the higher-level global warming scenarios (Abiodun et al., 2019; Naik and Abiodun, 2020). Other studies have equally demonstrated an increased drought incidence in future across various regions (e.g Wehner et al., 2011; Duffy et al., 2015; Huang et al., 2018; Ahmadalipour et al., 2017a, 2017b, 2019; Nguvava et al., 2019). This calls for continuous evaluation of drought extremes based on varying indices and improved quality of datasets in order to accurately simulate its evolution and develop appropriate adaptation measure across the sub-Saharan region.

4. Discussions

Due to lack of minimum/maximum temperature datasets that are necessary in computing the PET, this study used precipitation-based drought index to show projected changes. This is in line with other existing studies conducted over broader East Africa to show the future changes in drought and pluvial events based on SPI or/and SPEI (Nguvava et al., 2019; Spinoni et al., 2020; Haile et al., 2020). However, the conclusion of these studies has reported the better performance of SPEI as compared to SPI due to the PET inclusion. For instance, Nguvava et al. (2019) compared performance of two drought indices, namely SPI and SPEI. The study reported underestimation of drought frequency, severity, and intensity when employing SPI index as compared to the robust performance of SPEI. The findings of underestimation of SPI in projecting the changes in drought characteristics are equally noted in another study over Western Cape in South Africa (Naik and Abiodun, 2020). Spinoni et al. (2020), in a study focusing on future meteorological drought hotspots at global level based on CORDEX data and employing a number of drought indices, including SPI, showed that SPI estimates that about 15% of the global land is likely to experience more frequent and severe drought during RCP 4.5/8.5 while SPEI gives projections of about 49% under RCP 8.5 and (about 47%) under RCP 4.5.

Despite the variation in projections of drought, one fundamental agreement that models and indices show is an increase in drought incidences across the SPI spectrum as compared to the baseline period. However, as agreed in most literature, caution should be applied when employing precipitation-based indices only like SPI, since it does not account for temperature component that has continued to exhibit positive trajectory globally. Going forward, the next paradigm of research frontier regarding drought scenario should focus on addressing

fundamental questions such as those raised in study by Van Loon et al. (2016) and AghaKouchak et al. (2020). This study thus recommends in-depth understanding on the role of humans in aggravating the projected droughts especially in regions that were less considered as hotspots. Moreover, further studies should endeavor to investigate innovative mechanism on how to cope with excepted impact of drought on agriculture, energy sector, and human water use. This will cushion society and infrastructure from the adverse impacts and enable attainment of sustainable development goals.

5. Conclusion

The present study evaluates drought events by characterizing the operational features that identify drought's beginning, end and degree of severity. Examples of such features analyzed entailed: drought frequency, severity, intensity and duration. Meanwhile, the study used precipitated based index of SPI to evaluate future changes of drought over Kenya. SPI is useful index for examining the variability of dryness/wetness conditions due to its capacity to represent precipitation anomalies. In this study, the changes in annual and seasonal precipitation over Kenya are examined in order to associate with changes in drought occurrence. Here, the study employed various statistical models to assess the climatic variable employed in this study. Results for future rainfall changes demonstrate positive shift, indicating an increase in projected rainfall change during all the three timescales. Most of the changes in variance are statistically insignificant at 95% confidence level, except for RCP4.5 scenario during mid-term (2040–2069) for OND. On the drought projections, the results of the current study demonstrate relatively better performance of biased corrected MME derived from RCA4 models in simulating drought indices over the Kenya. The MME predict an increase in moderate drought incidences with fewer incidences of extreme events across all the RCPs and time slice under investigation. However, the duration of occurrences varies from one region to another with most hotspots located around northeastern sides of the country. However, it should be noted that more wet scenarios are depicted during the extreme and severe drought events, with fewer cases of drought events expected to occur during the projection period. For instance, the SPI-3 exhibits greater temporal frequencies of the occurrence for wet and dry cases during the last time slice during 2070–2100 under RCP8.5. The present study was limited to highlighting the projected changes in drought occurrence. Future studies should however focus on examining the causes and drivers of compound and cascading hazards over the study region.

Declaration of Competing Interest

In a unanimous agreement, all authors declare no conflict of interest in the present study.

Acknowledgments

The authors acknowledge Nanjing University of Information Science and Technology (NUIST) for providing favorable environment and infrastructural needs for conducting research. National Key Research and Development Program of China (2016YFA0600702), National Natural Science Foundation of China (41625019) supported this work. Special appreciation to all data centers for availing data to use for evaluation studies. The three anonymous reviewers are highly appreciated for the great input that led to the massive improvement of this manuscript.

References

Abiodun, B.J., Pal, J.S., Afiesimama, E.A., Gutowski, W.J., Adedoyin, A., 2008. Simulation of West African monsoon using RegCM3 Part II: impacts of deforestation and desertification. Theor. Appl. Climatol. 93, 245–261. https://doi.org/10.1007/s00704-007-0333-1.

Abiodun, B.J., Makhanya, N., Petja, B., Abatan, A.A., Oguntunde, P.G., 2019. Future projection of droughts over major river basins in Southern Africa at specific global warming levels. Theor. Appl. Climatol. 137, 1785–1799. https://doi.org/10.1007/s00704-018-2693-0.

Abrha, H., Hagos, H., 2019. Future drought and aridity monitoring using multi-model approach under climate change in Hintalo Wejerat district, Ethiopia. Sustain. Water Resour. Manag. 5, 1963–1972. https://doi.org/10.1007/s40899-019-00350-1.

AghaKouchak, A., Chiang, F., Huning, L.S., Love, C.A., Mallakpour, I., Mazdiyasni, O., Moftakhari, H., Papalexiou, S.M., Ragno, E., Sadegh, M., 2020. Climate extremes and compound hazards in a warming world. Annu. Rev. Earth Planet. Sci. 48 (20), 1–20.30.

Ahmadalipour, A., Moradkhani, H., Svoboda, M., 2017a. Centennial drought outlook over the CONUS using NASA-NEX downscaled climate ensemble. Int. J. Climatol. 37, 2477–2491. https://doi.org/10.1002/joc.4859.

Ahmadalipour, A., Moradkhani, H., Demirel, M.C., 2017b. A comparative assessment of projected meteorological and hydrological droughts: elucidating the role of temperature. J. Hydrol. 553, 785–797. https://doi.org/10.1016/j.jhydrol.2017.08.047.

Ahmadalipour, A., Moradkhani, H., Castelletti, A., Magliocca, N., 2019. Future drought risk in Africa: integrating vulnerability, climate change, and population growth. Sci. Total Environ. 662, 672–686. https://doi.org/10.1016/j.scitotenv.2019.01.278.

Ayugi, B.O., Tan, G., 2019. Recent trends of surface air temperatures over Kenya from 1971 to 2010. Meteorog. Atmos. Phys. 131, 1401–1413. https://doi.org/10.1007/s00703-018-0644-z.

Ayugi, B., Tan, G., Niu, R., Dong, Z., Ojara, M., Mumo, L., Hassen, B., Ongoma, V., 2020a. Evaluation of meteorological droughts and wet scenarios over Kenya, East Africa. Atmosphere 2020 (11), 307. https://doi.org/10.3390/atmos11030307.

Ayugi, B., Tan, G., Gnitou, G.T., Ojara, M., Ongoma, V., 2020b. Historical evaluations and simulations of precipitation over Eastern Africa from Rossby centre regional climate model. Atmos. Res. 232 10.1016.jatmosres.2019.104705.

Ayugi, B., Tan, G., Niu, R., Babaousmail, H., Ojara, M., Wido, H., Mumo, L., Nooni, I., Ongoma, V., 2020c. Quantile mapping bias correction on Rossby Centre regional models climate models for precipitation analysis over Kenya, East Africa. Preprints 2019. https://doi.org/10.3390/w120801.

Balint, Z., Mutua, F.M., Muchiri, P., 2011. Drought Monitoring with the Combined Drought Index. FAO-Swalim, Nairobi, Kenya, pp. 3–25.

Beguería, S., Vicente-Serrano, S.M., Reig, F., Latorre, B., 2014. Standardized precipitation evapotranspiration index (SPEI) revisited: parameter fitting, evapotranspiration models, tools, datasets and drought monitoring. Int. J. Climatol. 34, 3001–3023. https://doi.org/10.1002/joc.3887.

Behera, S.K., Luo, J.-J., Masson, S., Delecluse, P., Gualdi, S., Navarra, A., Yamagata, T., 2005. Paramount impact of the Indian Ocean dipole on the East African short rains: A CGCM study. J. Clim. 18, 4514–4530. https://doi.org/10.1175/JCLI3541.1.

Bonsal, B.R., Aider, R., Gachon, P., Lapp, S., 2013. An assessment of Canadian prairie drought: past, present, and future. Clim. Dyn. 41, 501–516. https://doi.org/10.1007/s00382-012-1422-0.

Burke, E.J., Brown, S.J., 2008. Evaluating uncertainties in the projection of future drought. J. Hydrometeorol. 9, 292–299. https://doi.org/10.1175/2007JHM929.1.

Camberlin, P., 2017. Temperature trends and variability in the Greater Horn of Africa: interactions with precipitation. Clim. Dyn. 48, 477–498. https://doi.org/10.1007/s00382-016-3088-5.

Camberlin, P., 2018. Climate of Eastern Africa. vol. 1https://doi.org/10.1093/acrefore/9780190228620.013.512.

Camberlin, P., Okoola, R.E., 2003. The onset and cessation of the “long rains” in eastern Africa and their interannual variability. Theor. Appl. Climatol. 54, 43–54. https://doi.org/10.1007/s00704-002-0721-5.

Carrão, H., Naumann, G., Barbosa, P., 2018. Global projections of drought hazard in a warming climate: a prime for disaster risk management. Clim. Dyn. 50, 2137–2155. https://doi.org/10.1007/s00382-017-3740-8.

Changwony, C., Sichangi, A.W., Murimi Ngigi, M., 2017. Using GIS and remote sensing in assessment of water scarcity in Nakuru County, Kenya. Adv. Remote Sens. 6, 88–102. https://doi.org/10.4236/ars.2017.61007.

Christensen, J.H., Boberg, F., Christensen, O.B., Lucas, P.P., 2008. On the need for bias correction of regional climate change projections of temperature and precipitation. Geophys. Res. Lett. 35, L20709. https://doi.org/10.1029/2008GL035694.

Christensen, J.H., Kanikicharla, K.K., Aldrian, E., An, S.I., Cavalcanti, I.F.A., De Castro, M., Dong, P., Goswami, A., Hall, Kanyanga, J.K., Kossin, J., Lau, N.-C., Renwick, J., Stephenson, D.B., Xie, S.-P., Zhou, T., Kitoh, A., 2013. Climate phenomena and their relevance for future regional climate change. In: Climate Change 2013 the Physical Science Basis: Working Group I Contribution to the Fifth Assessment Report of the Intergovernmental Panel on Climate Change. Cambridge University Press, pp. 1217–1308. https://doi.org/10.1017/CBO9781107415324.028.

Christy, J.R., Norris, W.B., McNider, R.T., 2009. Surface temperature variations in East Africa and possible causes. J. Clim. 22, 3342–3356. https://doi.org/10.1175/2008JCLI2726.1.

Collins, J.M., 2011. Temperature variability over Africa. J. Clim. 24, 3649–3666. https://doi.org/10.1175/2011JCLI3753.1.

Dai, A., 2011a. Characteristics and trends in various forms of the palmer drought severity index during 1900-2008. J. Geophys. Res. 116. https://doi.org/10.1029/2010JD015541.

Dai, A., 2011b. Drought under global warming: a review. WIRES Clim. Change 2, 45–65. https://doi.org/10.1002/wcc.81.

Dai, Aiguo, 2013. Increasing drought under global warming in observations and models. Nat. Clim. Chang. 3, 52–58. https://doi.org/10.1038/nclimate1633.

Dai, A., Zhao, T., Chen, J., 2018. Climate change and drought: a precipitation and evaporation perspective. Curr. Clim. Change Rep. 4, 301–312. https://doi.org/10.1007/

s40641-018-0101-6.
Dike, V.N., Shimizu, M.H., Diallo, M., Lin, Z., Nwofor, O.K., Chineke, T.C., 2015. Modelling present and future African climate using CMIP5 scenarios in HadGEM2-ES. Int. J. Climatol. 35, 1784–1799. https://doi.org/10.1002/joc.4084.
Duffy, P.B., Brando, P., Asner, G.P., Field, C.B., 2015. Projections of future meteorological drought and wet periods in the amazon. PNAS 112, 13172–13177. https://doi.org/10.1073/pnas.1421010112.
Dutra, E., Di Giuseppe, F., Wetterhall, F., Pappenberger, F., 2013. Seasonal forecasts of droughts in African basins using the standardized precipitation index. Hydrol. Earth Syst. 17, 2359. https://doi.org/10.5194/hess-17-2359-2013.
Eckstein, D., Künzel, V., Schäfer, L., Winges, M., 2020. Global Climate Risk Index 2020. Germanwatch, Bonn.
Endris, H.S., Omondi, P., Jain, S., Lennard, C., Hewitson, B., Chang'a, L., Awange, J.L., Dosio, A., Ketiem, P., Nikulin, G., Panitz, H.-J., Büchner, M., Stordal, F., Tazalika, L., 2013. Assessment of the performance of CORDEX regional climate models in simulating East African rainfall. J. Clim. 26, 8453–8475. https://doi.org/10.1175/JCLI-D-12-00708.1.
Endris, H.S., Lennard, C., Hewitson, B., Dosio, A., Nikulin, G., Panitz, H.J., 2016. Teleconnection responses in multi-GCM driven CORDEX RCMs over Eastern Africa. Clim. Dyn. 46, 2821–2846. https://doi.org/10.1007/s00382-015-2734-7.
Endris, H.S., Lennard, C., Hewitson, B., Dosio, A., Nikulin, G., Artan, G.A., 2019. Future changes in rainfall associated with ENSO, IOD and changes in the mean state over Eastern Africa. Clim. Dyn. 52, 2029–2053. https://doi.org/10.1007/s00382-018-4239-7.
Engelbrecht, F., Adegoke, J., Bopape, M.J., Naidoo, M., Garland, R., Thatcher, M., McGregor, J., Katzfrey, J., Werner, M., Gatebe, C., 2015. Projections of rapidly rising surface temperatures over Africa under low mitigation. Environ. Res. Lett. 10, 085004. https://doi.org/10.1088/1748-9326/10/8/085004.
Frank, A., Armenski, T., Gocic, M., Popov, S., Popovic, L., Trajkovic, S., 2017. Influence of mathematical and physical background of drought indices on their complementarity and drought recognition ability. Atmos. Res. 194, 268–280. https://doi.org/10.1016/j.atmosres.2017.05.006.
Gebrechorkos, S.H., Hülsmann, S., Bernhofer, C., 2018. Evaluation of multiple climate data sources for managing environmental resources in East Africa. Hydrol. Earth Syst. Sci. 22, 4547–4564. https://doi.org/10.5194/hess-2017-558.
Giannini, A., Saravanan, R., Chang, P., 2005. Dynamics of the boreal summer African monsoon in the NSIPP1 atmospheric model. Clim. Dyn. 25, 517–535. https://doi.org/10.1007/s00382-005-0056-x.
Gidey, E., Dikinya, O., Sebego, R., Segosebe, E., Zenebe, A., 2018. Predictions of future meteorological drought hazard (~ 2070) under the representative concentration path (RCP) 4.5 climate change scenarios in Raya, Northern Ethiopia. Model Earth Syst. Environ. 4, 475–488. https://doi.org/10.1007/s40808-018-0453-x.
Haile, G.G., Tang, Q., Hosseini-Moghari, S.M., Liu, X., Gebremicael, T.G., Leng, G., Kebde, A., Yun, X., 2020. Projected impacts of climate change on drought patterns over East Africa. Earth's Future. https://doi.org/10.11029/2020EF001502.
Hamed, K.H., Rao, R.A., 1998. A modified Mann–Kendall trend test for autocorrelated data. J. Hydrol. 204, 182–196.
Hastenrath, S., Polzin, D., Camberlin, P., 2004. Exploring the predictability of the 'short rains' at the coast of East Africa. Int. J. Climatol. 24, 1333–1343. https://doi.org/10.1002/joc.1070.
Hastenrath, S., Polzin, D., Mutai, C., 2011. Circulation mechanisms of Kenya rainfall anomalies. J. Clim. 24: 404–412. dio:https://doi.org/10.1175/2010JCLI3599.1.
Hayes, M.J., Svoboda, M.D., Wilhite, D.A., Vanyarkho, O.V., 1999. Monitoring the 1996 drought using the standardized precipitation index. Bull. Am. Meteorol. Soc. 80, 429–438.
Hirsch, R., Helsel, D., Cohn, T., Gilroy, E., 1993. Statistical analysis of hydrologic data. In: Maidment, D. (Ed.), Handbook of Hydrology. McGraw-Hill, New York.
Hoerling, M., Hurrell, J., Eischeid, J., Phillips, A., 2006. Detection and attribution of twentieth-century northern and southern African rainfall change. J. Clim. 19, 3989–4008.
Huang, J., Yu, H., Guan, X., Wang, G., Guo, R., 2016. Accelerated dryland expansion under climate change. Nat. Clim. Chang. 6, 166–171. https://doi.org/10.1038/NCLIMATE2837.
Huang, J., Zhai, J., Jiang, T., Wang, Y., Li, X., Wang, R., Xiong, M., Su, B., Fischer, T., 2018. Analysis of future drought characteristics in China using the regional climate model CCLM. Clim. Dyn. 50, 507–525. https://doi.org/10.1007/s00382-017-3623-z.
Hulme, M., 1992. Rainfall changes in Africa: 1931–1960 to 1961–1990. Int. J. Climatol. 12, 685–699. https://doi.org/10.1002/joc.3370120703.
Huning, L.S., AghaKouchak, A., 2018. Mountain snowpack response to different levels of warming. PNAS 115, 10932–10937. https://doi.org/10.1073/pnas.1805953115.
Indeje, M., Semazzi, F.H.M., Ogallo, L.J., 2000. ENSO signals in East African rainfall seasons. Int. J. Climatol. 20, 19–46. https://doi.org/10.1002/(SICI)1097-0088(200001)20:1<19.. AID-JOC449 > 3.0.CO;2-0.
Intergovernmental Panel on Climate Change, 2018. Global Warming of 1.5° C: An IPCC Special Report on the Impacts of Global Warming of 1.5° C Above Pre-industrial Levels and Related Global Greenhouse Gas Emission Pathways, in the Context of Strengthening the Global Response to the Threat of Climate Change, Sustainable Development, and Efforts to Eradicate Poverty. Intergovernmental Panel on Climate Change.
Ionita, M., Scholz, P., Chelcea, S., 2016. Assessment of droughts in Romania using the standardized Precipitation Index. Nat. Hazards 81, 1483–1498.
Jung, I.W., Chang, H., 2012. Climate change impacts on spatial patterns in drought risk in the Willamette River Basin, Oregon, USA. Theor. Appl. Climatol. 108, 355–371. https://doi.org/10.1007/s00704-011-0531-8.
Karanja, A., Ondimu, K., Recha, C., 2017. Analysis of temporal drought characteristic using SPI drought index based on rainfall data in Laikipia West Sub-County, Kenya. OALib 4, 1–11. https://doi.org/10.4236/oalib.1103765.
Kendall, M.G., 1975. Rank Correlation Methods, 4th ed. Griffin, London (202 pp).
Kent, C., Chadwick, R., Rowell, D.P., 2015. Understanding uncertainties in future projections of seasonal tropical precipitation. J. Clim. 28, 4390–4413.
Kerandi, N., Arnault, J., Laux, P., Wagner, S., Kitheka, J., Kunstmann, H., 2018. Joint atmospheric-terrestrial water balances for East Africa: a WRF-Hydro case study for the upper Tana River basin. Theor. Appl. Climatol. 131, 1337–1355. https://doi.org/10.1007/s00704-017-2050-8.
King'uyu, S.M., Ogallo, L.A., Anyamba, E.K., 2000. Recent trends of minimum and maximum surface temperatures over Eastern Africa. J. Clim. 13, 2876–2886. https://doi.org/10.1175/1520-0442(2000)013<2876:RTOMAM>2.0.CO;2.
Kisembe, J., Favre, A., Dosio, A., Lennard, L., Sabiiti, G., Nimusiima, A., 2018. Evaluation of rainfall simulations over Uganda in CORDEX regional climate models. Theor. Appl. Climatol. 137, 1117–1134. https://doi.org/10.1007/s00704-018-2643-x.
Liebmann, B., Hoerling, M.P., Funk, C., Bladé, I., Dole, R.M., Allured, D., Quan, X., Pegion, P., Eischeid, J.K., 2014. Understanding recent Eastern Horn of Africa rainfall variability and change. J. Clim. 27, 8630–8645. https://doi.org/10.1175/JCLI-D-13-00714.1.
Lyon, B., Dewitt, D.G., 2012. A recent and abrupt decline in the East African long rains. Geophys. Res. Lett. 39 (2), L02702. https://doi.org/10.1029/2011GL050337.
Maidment, R.I., Allan, R.P., Black, E., 2015. Recent observed and simulated changes in precipitation over Africa. Geophys. Res. Lett. 42, 8155–8164. https://doi.org/10.1002/2015GL065765.
Manatsa, D., Mukwada, G., Siziba, E., Chinyanganya, T., 2010. Analysis of multi-dimensional aspects of agricultural droughts in Zimbabwe using the standardized precipitation index (SPI). Theor. Appl. Climatol. 102, 287–305. https://doi.org/10.1007/s00704-010-0262-2.
Manatsa, D., Morioka, Y., Behera, S.K., Matarira, C.H., Yamagata, T., 2014. Impact of Mascarene high variability on the East African 'short rains'. Clim. Dyn. 42, 1259–1274. https://doi.org/10.1007/s00382-013-1848-z.
Mann, H.B., 1945. Non-parametric tests against trend. Econometrica 13, 245–259.
McKee, T.B., Doesken, N.J., Kleist, J., 1993. Drought monitoring with multiple time scales. In: 9th Conference on Applied Climatology. Amer. Meteorol. Soc, Dallas, TX, pp. 233–236.
Moss, R.H., Edmonds, J.A., Hibbard, K.A., Manning, M.R., Rose, S.K., Van Vuuren, D.P., Carter, T.R., Emori, S., Kainuma, M., Kram, T., Meehl, G.A., Mitchell, J.F.B., Nakicenovic, N., Riahi, K., Smith, S.J., Stouffer, R.J., Thomson, A.M., Weyant, J.P., Wilbanks, T.J., 2010. The next generation of scenarios for climate change research and assessment. Nature 463, 747–756. https://doi.org/10.1038/nature08823.
Mote, P. W., Li, S., Lettenmaier, D. P., Xiao, M., Engel, R., 2018. Dramatic declines in snowpack in the western US. Npj Clim. Atmos. Sci., 1.dio.https://doi.org/10.1038/s41612-018-0012-1.
Mutsotso, R.B., Sichangi, A.W., Makokha, G.O., 2018. Spatio-temporal drought characterization in Kenya from 1987 to 2016. Adv. Remote Sens. 07, 125–143. https://doi.org/10.4236/ars.2018.72009.
Mutundu, K.K., Nderitu, J.H., Mureithi, D., Wainaina, H., Ayugi, B., 2013. Baseline Survey on Interventions in Upgrading Animal Health and Production in through Training and Capacity Building in the ASALs of Marsabit.
Naik, M., Abiodun, B.J., 2020. Projected changes in drought characteristics over the Western Cape, South Africa. Meteorol. Appl. 27, 1–15. https://doi.org/10.1002/met.1802.
Nguvava, M., Abiodun, B.J., Otieno, F., 2019. Projecting drought characteristics over East African Basins at specific global warming levels. Atmosres 228, 41–54. https://doi.org/10.1016/j.atmosres.2019.05.008.
Nicholson, S.E., 2000. The nature of rainfall variability over Africa on time scales of decades to millenia. Glob. Plan. Chang. 26, 137–158.
Nicholson, S.E., 2008. The intensity, location and structure of the tropical rainbelt over West Africa as factors in interannual variability. Int. J. Climatol. l28, 1775–1785. https://doi.org/10.1002/joc.1507.
Nicholson, S.E., Kim, J., 1997. The relationship of the El Niño–Southern Oscillation to African rainfall. Int. J. Climatol. 17 (2), 117–135. https://doi.org/10.1002/(SICI)10970088(199702)17:2<117::AID-JOC84>3.0.CO;2-O.
Nogherotto, R., Coppola, E., Giorgi, F., Mariotti, L., 2013. Impact of Congo Basin deforestation on the African monsoon. Atmos. Sci. Lett. 14, 45–51. https://doi.org/10.1002/asl2.416.
Ogwang, Chen, H., Li, X., Gao, 2014. The influence of topography on East African October to December climate: sensitivity experiments with RegCM4. Adv. Meteorol. 2014https://doi.org/10.1155/2014/143917. ID 14917.
Omondi, P.A., Awange, J.L., Forootan, E., Ogallo, L.A., Barakiza, R., Girmaw, G.B., Fesseha, I., Kululetera, V., Kilembe, C., Mbati, M.M., Kilavi, M., King'uyu, S.M., Omeny, P.A, Njogu, A., Badr, E.M., Musa, T.A., Muchiri, P., Bamanya, D., Komutunga, E., 2014. Changes in temperature and precipitation extremes over the Greater Horn of Africa region from 1961 to 2010. Int. J. Climatol., 34: 1262–1277. doi:https://doi.org/10.1002/joc.3763.
Ongoma, V., Chen, H., Gao, C., Sagero, P.O., 2017. Variability of temperature properties over Kenya based on observed and reanalyzed datasets. Theor. Appl. Climatol. 133, 1175–1190. https://doi.org/10.1007/s00704-017-2246-y.
Ongoma, V., Chen, H., Gao, C., 2018a. Projected change in mean rainfall and temperature over East Africa based on CMIP5 models. Int. J. Climatol. 38, 1375–1392. https://doi.org/10.1002/joc.5252.
Ongoma, V., Chen, H., Gao, C., Nyongesa, A.M., Polong, F., 2018b. Future changes in climate extreme over equatorial East Africa based on CMIP5 multimodel ensemble. Nat. Hazards 90, 901–920. https://doi.org/10.1007/s11069-017-3079-9.
Peel, M.C., Finlayson, B.L., Mcmahon, T.A., 2007. Updated world map of the Koppen-Geiger climate classification. Hydrol. Earth Syst. Sci. 11, 1633–1644.
Philippon, N., Camberlin, P., Fauchereau, N., 2002. Empirical predictability study of

October–December east African rainfall. Q.J.R: Meteorol. Soc 128 (585), 2239–2256. https://doi.org/10.1256/qj.01.190.
Polong, F., Chen, H., Sun, S., Ongoma, V., 2019. Temporal and spatial evolution of the standard precipitation evapotranspiration index (SPEI) in the Tana River Basin , Kenya. Theor. Appl. Climatol. 138 (1–2), 777–792. https://doi.org/10.1007/s00704-019-02858-0.
Prudhomme, C., Giuntoli, I., Robinson, E.L., Clark, D.B., Arnell, N.W., Dankers, R., Fekete, B.M., Fransen, W., Gerten, D., Gosling, S.N., Hagemann, S., Kim, H., Maski, Y., Satoh, Y., Stacke, T., Wada, Y., Wisser, D., 2014. Hydrological droughts in the 21st century, hotspots and uncertainties from a global multimodel ensemble experiment. PNAS 111 (9), 3262–3267. https://doi.org/10.1073/pnas.1222473110.
Reliefweb, 2019. Kenya: Drought. 2014–2019. Available at: https://reliefweb.int/disaster/dr-2014-000131-ken.
Riahi, K., Rao, S., Krey, V., Cho, C., Chirkov, V., Fischer, G., Kindermann, G., Nakicenovic, N., Rafaj, P., 2011. RCP 8.5-A scenario of comparatively high greenhouse gas emissions. Clim. Chang. 109, 33–57. https://doi.org/10.1007/s10584-011-0149-y.
Richard, Y., Fauchereau, N., Poccard, I., Rouault, M., Trzaska, S., 2001. 20th century droughts in southern Africa: spatial and temporal variability, teleconnections with oceanic and atmospheric conditions. Int. J. Climatol. 21, 873–885. https://doi.org/10.1002/joc.656.
Rowell, D.P., Booth, B.B.B., Nicholson, S.E., Good, P., 2015. Reconciling past and future rainfall trends over East Africa. J. Clim. 28, 9768–9788. https://doi.org/10.1175/JCLI-D-15-0140.1.
Saji, N.H., Goswami, B.N., Vinayachandran, P.N., Yamagata, T., 1999. A dipole mode in the tropical Indian Ocean. Nature 401, 360–363. https://doi.org/10.1038/43854.
Samuelsson, P., Jones, C.G., Willén, U., Ullerstig, A., Gollvik, S., Hansson, U., Hansson, U., Jansson, C., Kjellströ, E., Nikulin, G., Wyser, K., 2012. The Rossby Centre regional climate model RCA3: model description and performance. Tellus A 63, 4–23. https://doi.org/10.1111/j.1600-0870. 2010.00478.x.
Schreck, C.J., Semazzi, F.H.M., 2004. Variability of the recent climate of eastern Africa. Int. J. Climatol. 24, 681–701. https://doi.org/10.1002/joc.1019.
Sen, P.K., 1968. Estimates of the regression coefficient based on Kendall's Tau. J. Am. Stat. Assoc. 63, 1379–1389. https://doi.org/10.2307/2285891.
Sheffield, Justin, Wood, Eric F., 2008. Projected changes in drought occurrence under future global warming from multi-model, multi-scenario, IPCC AR4 simulations. Clim. Dyn. 31, 79–105. https://doi.org/10.1007/s00382-007-0340-z.
Sheffield, J., Wood, E.F., 2007. Characteristics of global and regional drought, 1950–2000: analysis of soil moisture data from off-line simulation of the terrestrial hydrologic cycle. J. Geophys. Res. 112 (D17). https://doi.org/10.1029/2006JD008288.
Sheffield, J., Wood, E.F., Roderick, M.L., 2012. Little change in global drought over the past 60 years. Nature 491, 435–438. https://doi.org/10.1038/nature11575.
Shem, O.W., Dickinson, R.E., 2006. How the Congo basin deforestation and the equatorial monsoonal circulation influences the regional hydrological cycle. In: Proc of the 86th Annu Americ Meteorol Soc Meeting. vol. 31.
Shongwe, M.E., Van Oldenborgh, G.J., Van den Hurk, B., Van Aalst, M., 2011. Projected changes in mean and extreme precipitation in Africa under global warming. Part II: East Africa. J. Climate 24, 3718–3733. https://doi.org/10.1175/2010JCLI2883.1.
Skiles, S.M., Flanner, M., Cook, J.M., Dumont, M., Painter, T.H., 2018. Radiative forcing by light-absorbing particles in snow. Nat. Clim. Chang., 8, 964-971.dio.https://doi.org/10.1038/s41558-018-0296-5.
Sneyers, R., 1990. On the Statistical Analysis of a Series of Observations. Tech. Note 143, WMO-No. 415. pp. 192.
Spinoni, J., Naumann, G., Carrao, H., Barbosa, P., Vogt, J., 2014. World drought frequency, duration, and severity for 1951–2010. Int. J. Climatol. 34, 2792–2804. https://doi.org/10.1002/joc.3875.
Spinoni, J., Barbosa, P., Bucchignani, E., Cxassano, J., Cavazos, T., Christensen, H., Coppola, E., Evans, J., Geyer, B., Giorgi, F., Hadjinicolaou, P., Jacob, D., Katzfey, J., Koenigk, T., Laprise, R., Lennard, C.J., Kurnaz, L.M., Li, D., Llopart, M., McCormic, N., Naumann, G., Nikilun, G., Ozturk, T., Juergen, H.P., Porfirio, D.R., Rockel, B., Solman, S.A., Syktus, J., Tangng, F., Teichmann, C., Vautard, R., Vogt, J., Winger, K., Zittis, G., Alessandro, D., 2020. Future global meteorological drought hotspots: a study based on CORDEX data. J. Clim. https://doi.org/10.1175/JCLI-D-19-0084.1.
Strandberg, G., Bärring, L., Hansson, U., Jansson, C., Jones, C., Kjellström, E., Kolax, M., Kupiainen, M., Nikulin, G., Samuelsson, P., 2015. CORDEX Scenarios for Europe from the Rossby. Centre Regional Climate Model RCA4; Report Meteorology and Climatology No. 116. Swedish Meteorological and Hydrological Institute, Norrköping, Sweden.
Sun, F., Roderick, M. L., Lim, W. H., Farquhar, G.D., 2011. Hydroclimatic projections for the Murray-Darling Basin based on an ensemble derived from intergovernmental panel on climate change AR4 climate models. Water Resour. Res. 47(12).dio:https://doi.org/10.1029/2010WR009829.
Tierney, J.E., Ummenhofer, C.C., deMenocal, P.B., 2015. Past and future rainfall in the Horn of Africa. Sci. Adv. 1, e1500682. https://doi.org/10.1126/sciadv.1500682.
Touma, D., Ashfaq, M., Nayak, M.A., Kao, S.C., Diffenbaugh, N.S., 2015. A multi-model and multi-index evaluation of drought characteristics in the 21st century. J. Hydrol. 526, 196–207. https://doi.org/10.1016/j.jhydrol.2014.12.011.
Trenberth, K.E., Dai, A., Van Der Schrier, G., Jones, P.D., Barichivich, J., Briffa, K.R., Sheffield, J., 2014. Global warming and changes in drought. Nat. Clim. Chang. 4, 17–22. https://doi.org/10.1038/NCLIMATE2067.
Ukkola, A.M., Pitman, A.J., De Kauwe, M.G., Abramowitz, G., Herger, N., Evans, J.P., Decker, M., 2018. Evaluating CMIP5 model agreement for multiple drought metrics. J. Hydrometeorol. 19, 969–988. https://doi.org/10.1175/JHM-D-17-0099.1.
Unden, P., Rontu, L., Jinen, H., Lynch, P., Calvo, J., Cats, G., Cuxart, J., Eerola, K., Fortelius, C., Garcia-Moya, J.A., Jones, C., Geert Lenderlink, G., Mcdonald, A., Mcgrath, R., Navascues, B., Nielsen, N.W., Degaard, V., Rodriguez, E., Rummukainen, M., Sattler, K., Sass, B.H., Savijarvi, H., Schreur, B.W., Sigg, R., 2002. HIRLAM-5 Scientific Documentation. https://repositorio.aemet.es/bitstream/20.500.11765/6323/1/HIRLAMSciDoc_Dec2002.pdf.
Van Loon, A.F., Stahl, K., Di Baldassarre, G., Clark, J., Rangecroft, S., Wanders, N., Gleeson, T., Albert, I.J.M., Tallaksen, L.M., Hannaford, J., Uijlenhoet, R., Teulin, A., Hannah, D., Sheffield, J., Svoboda, M., Verbeiren, B., Wagener, T., Lanen, H.A.J., 2016. Drought in a human-modified world: reframing drought definitions, understanding, and analysis approaches. Hydrol. Earth Syst. Sci. 20, 3631–3650. https://doi.org/10.5194/hess-20-3631-2016.
Vicente-Serrano, S.M., López-Moreno, J.I., 2005. Hydrological response to different time scales of climatological drought: an evaluation of the standardized Precipitation Index in a mountainous Mediterranean basin. Hydrol. Earth Syst. Sci. 9, 523–533.
Vicente-Serrano, S.M., Beguería, J., López-Moreno, 2010. A multiscalar drought index sensitive to global warming: the standardized precipitation evapotranspiration index. J. Clim. 23, 1696–1718. https://doi.org/10.1175/2009JCLI2909.1.
Wambua, R.M., Benedict, M.M., James, M.R., 2018. Detection of spatial, temporal and trend of meteorological drought using standardized precipitation index (SPI) and effective drought index (EDI) in the Upper Tana River Basin, Kenya. Open J. Modern Hydrol. 8, 83–100. https://doi.org/10.4236/ojmh.2018.83007.
Wang, Z., Zhong, R., Lai, C., Zeng, Z., Lian, Y., Bai, X., 2018. Climate change enhances the severity and variability of drought in the Pearl River Basin in South China in the 21st century. Agr. Met 249, 149–162. https://doi.org/10.1016/j.agrformet.2017.12.077.
Wehner, M, Easterlin, D., Lawrimore, J.H., Heim, R., Vose, R., Santer, B., 2011. "Projections of future drought in the continental United States and Mexico." J. Hydrometeorol. 12,359–77. https://doi.org/10.1175/2011JHM1351.1.
Williams, A.P., Funk, C., 2011. A westward extension of the warm pool leads to a westward extension of the Walker circulation, drying eastern Africa. Clim. Dyn. 37, 2417–2435. https://doi.org/10.1007/s00382-010-0984-y.
World Bank, 2012. Doing Business in the East African Economies. 116 IFC/World Bank Rep.
Yang, W., Seager, R., Cane, M.A., Lyon, B., 2014. The East African long rains in observations and models. J. Clim. 27, 7185–7202. https://doi.org/10.1175/JCLI-D-13-00447.1.
Yang, W., Seager, R., Cane, M.A., Lyon, B., 2015. The annual cycle of East African precipitation. J. Clim. 28 (6), 2385–2404. https://doi.org/10.1175/JCLI-D-14-00484.1.
Zargar, A., Sadiq, R., Naser, B., Khan, F.I., 2011. A review of drought indices. Environ. Rev. 19, 333–349. https://doi.org/10.1139/a11-013.
Zhai, L., Feng, Q., 2009. Spatial and temporal pattern of precipitation and drought in Gansu Province, Northwest China. Nat. Hazards 49, 1–24. https://doi.org/10.1007/s11069-008-9274-y.
Zhao, T., Dai, A., 2017. Uncertainties in historical changes and future projections of drought. Part II: model-simulated historical and future drought changes. Clim. Chang. 144, 535–548. https://doi.org/10.1007/s10584-016-1742-x.